Inositol (1,4,5)-trisphosphate receptor links to filamentous actin are important for generating local Ca^{2+} signals in pancreatic acinar cells

Matthew R. Turvey[1], Kevin E. Fogarty[2] and Peter Thorn[1,*]

[1]Department of Pharmacology, University of Cambridge, Tennis Court Road, Cambridge, CB2 IPD, UK
[2]Biomedical Imaging Group, Department of Physiology, University of Massachusetts Medical School, Worcester, MA 01650, USA
*Author for correspondence (e-mail: pt207@cam.ac.uk)

Accepted 21 December 2004
Journal of Cell Science 118, 971-980 Published by The Company of Biologists 2005
doi:10.1242/jcs.01693

Summary

We explored a potential structural and functional link between filamentous actin (F-actin) and inositol (1,4,5)-trisphosphate receptors (IP_3Rs) in mouse pancreatic acinar cells. Using immunocytochemistry, F-actin and type 2 and 3 IP_3Rs (IP_3R2 and IP_3R3) were identified in a cellular compartment immediately beneath the apical plasma membrane. In an effort to demonstrate that IP_3R distribution is dependent on an intact F-actin network in the apical subplasmalemmal region, cells were treated with the actin-depolymerising agent latrunculin B. Immunocytochemistry indicated that latrunculin B treatment reduced F-actin in the basolateral subplasmalemmal compartment, and reduced and fractured F-actin in the apical subplasmalemmal compartment. This latrunculin-B-induced loss of F-actin in the apical region coincided with a reduction in IP_3R2 and IP_3R3, with the remaining IP_3Rs localized with the remaining F-actin. Experiments using western blot analysis showed that IP_3R3s are resistant to extraction by detergents, which indicates a potential interaction with the cytoskeleton. Latrunculin B treatment in whole-cell patch-clamped cells inhibited Ca^{2+}-dependent Cl^- current spikes evoked by inositol (2,4,5)-trisphosphate; this is due to an inhibition of the underlying local Ca^{2+} signal. Based on these findings, we suggest that IP_3Rs form links with F-actin in the apical domain and that these links are essential for the generation of local Ca^{2+} spikes.

Supplementary material available online at
http://jcs.biologists.org/cgi/content/full/118/5/971/DC1

Key words: Acinar, Actin, IP_3R, Ca^{2+}

Introduction

Pancreatic acinar cells are polarized epithelial cells that secrete fluid and enzymes in response to stimulation with agonists such as acetylcholine (ACh) and cholecystokinin (CCK) (Palade et al., 1975; Williams et al., 1997; Williams, 2001). Fluid and enzyme secretion in pancreatic acinar cells are Ca^{2+}-dependent processes (Petersen, 1992), which rely on agonist-evoked rises in intracellular Ca^{2+} that originate within the apical region of the cell (Kasai et al., 1993; Thorn et al., 1993). The apical region contains secretory vesicles termed zymogen granules, which fuse with the apical plasma membrane upon receiving a Ca^{2+} signal, releasing their contents into the luminal extracellular environment in a process of exocytosis (Giovannucci et al., 1998; Ito et al., 1997; Palade et al., 1975). In addition, Ca^{2+}-dependent Cl^- channels present in the apical plasma membrane, thought to be important in regulating fluid secretion, are activated by agonist-evoked rises in intracellular Ca^{2+} (Kasai and Augustine, 1990; Park et al., 2001).

Increases in intracellular Ca^{2+} emanate from regions near the apical plasma membrane, which coincides with the location of inositol (1,4,5)-trisphosphate receptors (IP_3Rs) (Fogarty et al., 2000a; Lee et al., 1997b; Nathanson et al., 1994; Yule et al., 1997). IP_3Rs are Ca^{2+}-release channels that are embedded in the membrane of the major intracellular Ca^{2+} store, namely the endoplasmic reticulum (ER), and are activated by the second messenger IP_3 (Berridge, 1993; Streb et al., 1983). It is likely that the localized distribution of IP_3Rs to the apical subplasmalemmal region ensures that Ca^{2+}-dependent processes that are known to occur within the apical region are able to function effectively. For example, it has been shown that cytosolic Ca^{2+} levels within the apical region must reach micromolar concentrations for exocytosis to occur (Ito et al., 1997; Stecher et al., 1992).

A previous study indicated that the cytoskeleton has an important role in maintaining Ca^{2+} signalling in pancreatic acinar cells. In this study it was shown that local Ca^{2+} spiking depends on the microtubular network to position the ER locally, and therefore Ca^{2+} release sites, within the apical region of pancreatic acinar cells (Fogarty et al., 2000b). Evidence from studies performed in a variety of cell types, including pancreatic cells, suggests that IP_3Rs link to the actin cytoskeleton and actin-associated proteins (Bourguignon et al., 1993a; Giovannucci et al., 2000; Joseph and Samanta, 1993; Rossier et al., 1991; Sugiyama et al., 2000; Tuvia et al., 1999). Furthermore, it has been shown that disrupting the actin cytoskeleton with actin depolymerising agents, impairs the ability of cells to raise cytosolic Ca^{2+} levels in response to either IP_3 or agonist stimulation, indicating that a link between IP_3Rs and the actin cytoskeleton is important for generating agonist-evoked Ca^{2+} signals in certain cell types (Bourguignon et al., 1993b; Shin et al., 2000).

Here, we examine the localization of the actin cytoskeleton and IP_3Rs in pancreatic acinar cells and the possible involvement of the actin cytoskeleton in IP_3-mediated Ca^{2+} release. Immunocytochemistry indicates that F-actin and IP_3Rs are contained within the same apical subplasmalemmal compartment. Treatment of the cells with the actin depolymerising agent latrunculin B caused a loss of F-actin at the basolateral plasma membrane and a reduction in F-actin and IP_3Rs in the apical domain. After latrunculin B treatment the remaining IP_3Rs were found localized in the same regions as the remaining F-actin. The actin cytoskeleton and IP_3Rs were both found to be present in a detergent insoluble pellet and disruption of the actin cytoskeleton disrupts local Ca^{2+} spikes. Our results suggest that F-actin in the apical domain of pancreatic acinar cells forms links with IP_3Rs and that this arrangement is important for generating local Ca^{2+} spikes in pancreatic acinar cells.

Materials and Methods

Drugs and antibodies

Latrunculin B was obtained from Alexis Biochemicals (Nottingham, UK). Rabbit anti-IP_3R2 polyclonal antibody (pAb) was obtained from Chemicon International (Temecula, CA). Mouse anti-IP_3R3 monoclonal antibody (mAb) was obtained from Transduction Laboratories, BD Biosciences (Lexington, KY). Rabbit anti-pan actin pAb was obtained from Cytoskeleton Inc. (Denver, CO). Mouse anti-β-actin mAb was obtained from Sigma (Poole, UK). Anti-mouse fluorescein isothiocyanate (FITC)-conjugated and anti-rabbit cyanine (Cy3)-conjugated secondary antibodies were obtained from Jackson Immunoresearch (West Grove, PA). AlexaFluor 546-phalloidin was obtained from Molecular Probes (Eugene, OR).

Preparation of pancreatic acini for confocal microscopy, electrophysiology and fluorescence imaging

Male outbred albino mice (25 g) were sacrificed humanely by cervical dislocation in accordance with UK Home Office regulations and the pancreas dissected. Mouse pancreatic acinar cells were prepared by CLSPA collagenase (Worthington, Lakewood, NJ) digestion at 37°C for 6 minutes as previously described (Thorn and Petersen, 1992). Cells were plated onto poly-L-ornithine-coated glass coverslips or plastic dishes and allowed to settle for a period of approximately 5 minutes.

Confocal microscopy

Preparation of cells for phalloidin staining was as follows. Cells attached to glass coverslips were washed quickly in PBS (including Ca^{2+} and Mg^{2+}) and then once in PIPES buffer, which contained (in mM): PIPES (dipotassium salt) 80, EGTA 5, $MgCl_2$ 2, pH to 7.4 with KOH. Cells were fixed in 4% paraformaldehdye in PIPES buffer for 30 minutes and then permeabilised in 0.1% Triton X-100 in PBS for 5 minutes. Cells were then incubated in Alexa Fluor 546 phalloidin for 30 minutes and then mounted on glass coverslips. Preparation of cells for immunofluorescence studies was as followed. Cells attached to glass coverslips were washed quickly in PBS and then fixed and permeabilised with cold methanol for 10 minutes at –20°C. After blocking for 1 hour in 2% donkey serum plus 2% fish skin gelatin in PBS, cells were incubated in primary antibody for 1 hour. The antibody dilutions were as follows: IP_3R2 (pAb), 1:20; IP_3R3 (mAb), 1:100; actin (pAb), 1:50-100; actin (mAb), 1:100. After washing, secondary antibodies conjugated to either a FITC fluorphore or a Cy3 fluorphore were applied for 30 minutes and then cells were mounted on glass coverslips. Images were obtained with a Zeiss Axiovert LSM510 confocal microscope fitted with a 63× planacromat, 1.4 NA, oil immersion objective. The FITC fluorphore was excited with an argon laser at 488 nm and the emitted light was captured after passing through a 505 nm long-pass filter. Alex Fluor 543 phalloidin and the Cy3 fluorphore were excited with a Helium-Neon laser at 543 nm and the emitted light was captured after passing through a 560 nm long-pass filter. Images were obtained as ten confocal sections separated in the z dimension by 1 μm. Images were deconvolved using Metamorph software (Universal Imaging Corporation).

In the experiments studying the effects of gelsolin, live cells were washed in PBS then permeabilized in a solution (BRB80) containing (mM): EGTA 1, $MgCl_2$ 1, PIPES 80, pH 6.8 plus 4% polyethylene glycol (mean M_r 8000) and 1% Trition X-100. Recombinant gelsolin (a gift from M. Schell, Department of Pharmacology, Cambridge University, UK) was then added to the media for 5 minutes prior to fixation in 4% paraformaldehdye.

Electrophysiology

The whole-cell configuration of the patch-clamp technique (Hamill et al., 1981) was used to record currents from single pancreatic acinar cells using a patch-clamp amplifier (EPC-9, HEKA, Lambrecht, Germany). Cells were plated on poly-L-ornithine-coated dishes and mounted on a Nikon TMS upright microscope. Patch-clamp pipettes were pulled from borosilicate glass capillaries (WPI, Sarasota, FL) on a Flaming/Brown micropipette puller (Model P-87, Sutter Instruments, Novato, CA). When filled with intracellular solution, pipettes had a resistance of 3-6 MΩ. After breaking through to the whole-cell configuration we accepted cells with an uncompensated series resistance of 10-25 MΩ. In all experiments the cells were whole-cell voltage-clamped at –30 mV and whole-cell currents were sampled at 2 kHz. The pipette solution contained (in mM): KCl 140, $MgCl_2$ 1.1, EGTA 0.1-0.2, HEPES 10, ATP 2, pH 7.2 with KOH, inositol (2,4,5)-trisphosphate [(2,4,5)IP_3] 0.01. The extracellular solution contained (in mM): NaCl 135, KCl 5, $MgCl_2$ 1, $CaCl_2$ 2, glucose 10, HEPES 10, pH 7.4 with NaOH. Drugs were added as boli to the bath solution. All experiments were conducted at room temperature (~21°C). The inclusion of 10 μM (2,4,5)IP_3 (a gift from R. F. Irvine, Cambridge University, UK) in the pipette solution elicited a train of short-lasting Ca^{2+}-dependent current spikes, previously shown to be a faithful reflection of Ca^{2+} release in the secretory pole of acinar cells (Thorn et al., 1993).

In the experiments of Fig. 6E, the intracellular solution contained a free concentration of Ca^{2+} of 600 nM, set by adding 10 mM EGTA and 7.88 mM $CaCl_2$ according to the computer algorithm MAXC. The current-voltage graph was produced using 1.5 second voltage steps from a holding potential of –30 mV to a range of potentials between –75 mV and +75 mV. The currents obtained showed the typical outward rectification for the Cl^- currents of pancreatic acinar cells (Kidd and Thorn, 2001) and the current amplitude was recorded at the end of the voltage step. Cells were treated with 100 μM latrunculin B for at least 5 minutes before recording the current-voltage relationship.

Fluorescence imaging

Ca^{2+} imaging experiments were performed by inclusion of 40-50 μM Calcium Green (Molecular Probes, Eugene, OR) in the pipette solution. Cells were illuminated with a visible laser (Coherent Innova 70) at 488 nm and imaged through a Nikon 40× UV, 1.3 NA, oil immersion objective. The emitted light was collected through a dichroic mirror (505DCLP; Chroma Technology, Brattleboro, VT) and filtered through a 510 nm long-pass filter (Chroma Technology). Full-frame images (128×128 pixels) were captured on a cooled CCD camera (70% quantum efficiency, 5 electrons readout noise; Massachusetts Institute of Technology (MIT), Lincoln Laboratories) with a pixel size of 200 nm at the specimen and at rates of up to 500 Hz (Fogarty et al., 2000a). Whole-cell patch-clamp data were simultaneously acquired using an Axopatch 200B patch-clamp amplifier with recording conditions as described above. After recording to a computer, the data were analysed with custom software with bleach correction routines and appropriate smoothing. Images were displayed in terms of $\Delta F/F_o$ [$100\times(F-F_o)/F_o$], where F is the recorded fluorescence and F_o was obtained from the mean of 20 sequential frames where no activity was apparent. The principle advantage of this imaging technique is the fast rate of acquisition of full frame images (Rizzuto et al., 1998).

Detergent extraction and western blotting

Male outbred albino mice (25 g) were sacrificed humanely by cervical dislocation in accordance with UK Home Office regulations and the pancreas dissected. Pancreatic tissue was dissociated with a surgical blade in ice-cold sucrose buffer containing (in mM): sucrose 340, EDTA 5, MOPS 20, pH 6.8, supplemented with protease inhibitors (8 μg/ml pepstatin, 8 μg/ml aprotinin, 8 μg/ml leupeptin, 1-1.6 mM benzamidine, and 1 mM PMSF). The dissociated tissue was homogenised in ice-cold sucrose buffer and then spun at 700 ***g*** for 10 minutes. The supernatant was collected and spun for a further 10 minutes at 2800 ***g***. The resulting pellet was resuspended in lysis buffer containing (in mM): Tris 50, pH 6.8, NaCl 150, EDTA 2, EGTA 2, and 0.5% (v/v) Triton X-100, supplemented with the aforementioned protease inhibitors, and gently agitated on a rotating wheel at 4°C for 1 hour. The lysate was cleared by centrifugation at 23,000 ***g*** to obtain a Triton X-100-soluble supernatant and Triton X-100-insoluble pellet (resuspended in lysis buffer). The Triton X-100-soluble and insoluble fractions were assayed for protein concentration. Proteins were separated by SDS-PAGE using 7.5% Tris-HCl polyacrylamide gels. The separated proteins were transferred to nitrocellulose membrane (Schleicher & Schuell, Dassel, Germany), and the blot was blocked for 1 hour at room temperature, on a shaker, in a solution containing Tris-buffered saline (20 mM Tris, pH 7.6, 137 mM NaCl), 0.1% (v/v) Tween 20 and 5% non-fat milk mix. The blot was cut into sections as required and incubated with primary antibody overnight at 4°C, with shaking in blocking solution. Antibodies to IP_3R3 and β-actin were both used at 1:1000. Immunoreactivity was observed using secondary antibodies conjugated to horseradish peroxidase followed by detection using a chemiluminescent reaction mixture (SuperSignal West Pico Chemiluminescent Substrate, Pierce Biotechnology, Rockford, IL) exposed on autoradiography film (Amersham Biosciences UK, Little Chalfont, UK).

Results

F-actin and IP_3Rs are enriched in the apical subplasmalemmal compartment

The lobules and fragments of mouse pancreatic tissue used consist of clusters of cells that retain the typical morphology of acinar cells in exocrine secretory end-pieces. Phalloidin staining of paraformaldehyde-fixed tissue fragments highlights the distribution of F-actin. As demonstrated in Fig. 1A, F-actin is located predominately in the cell apex, which in the tissue fragments appears as a thick, branching, band of F-actin running along the acini lumen. F-actin is also apparent in the lateral and basolateral subplasmalemmal regions but to a lesser degree. The distributions of IP_3R2 and IP_3R3 in pancreatic acinar cells were determined by immunocytochemistry. These

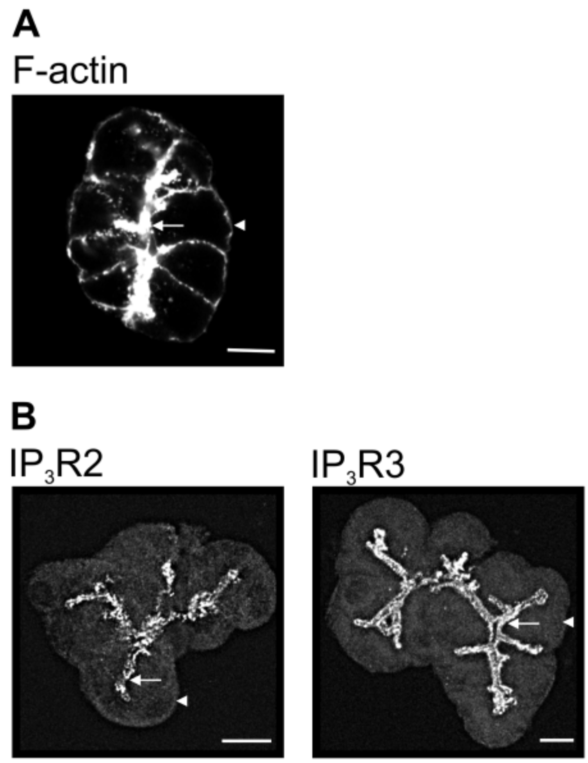

Fig. 1. F-actin and IP_3Rs are both contained within the apical subplasmalemmal compartment of pancreatic acini. Isolated pancreatic acinar cell clusters were fixed and stained with (A) phalloidin to highlight F-actin, or with (B) antibodies to IP_3R2 (pAb) and IP_3R3 (mAb). The image in A is a confocal section taken through the middle of the cell cluster. The images in B are 10 confocal serial sections separated by approximately 1 μm in the z-axis projected onto a single plane. Arrows denote the apical membrane and arrowheads denote the basolateral membrane. Bar, 10 μm.

receptor subtypes are the predominant forms in pancreas [as a percentage of total IP_3R: 53% IP_3R2 and 44% IP_3R3 (Wojcikiewicz, 1995)]. Cell clusters were methanol-fixed and stained with antibodies to IP_3R2 and IP_3R3. As can be seen in Fig. 1B, both types of IP_3Rs are predominately located in the cell apex. In cell clusters this appears as a branching network running along the acini lumen. These images demonstrate that F-actin and IP_3R2 and IP_3R3 are both present in a region immediately beneath the apical plasma membrane. All images are representative of acquisitions from at least seven separate preparations. The data on IP_3R distribution are consistent with previous data (Lee et al., 1997b; Yule et al., 1997), but using 3D reconstruction of pancreatic fragments (as opposed to tissue sections) we show for the first time the remarkable branching pattern of IP_3Rs within an acinus (see supplementary material Movie 1).

Experiments were performed to determine F-actin and IP_3R distribution in the same cell cluster. As the best demonstration of IP_3R distribution was achieved with methanol fixation, and methanol treatment of the actin cytoskeleton destroys the phalloidin-binding site, an antibody to actin rather than phalloidin was used to highlight the actin cytoskeleton. Staining with actin antibodies is expected to label both G-actin and F-actin and, consistent with that, some immunostaining

Journal of Cell Science

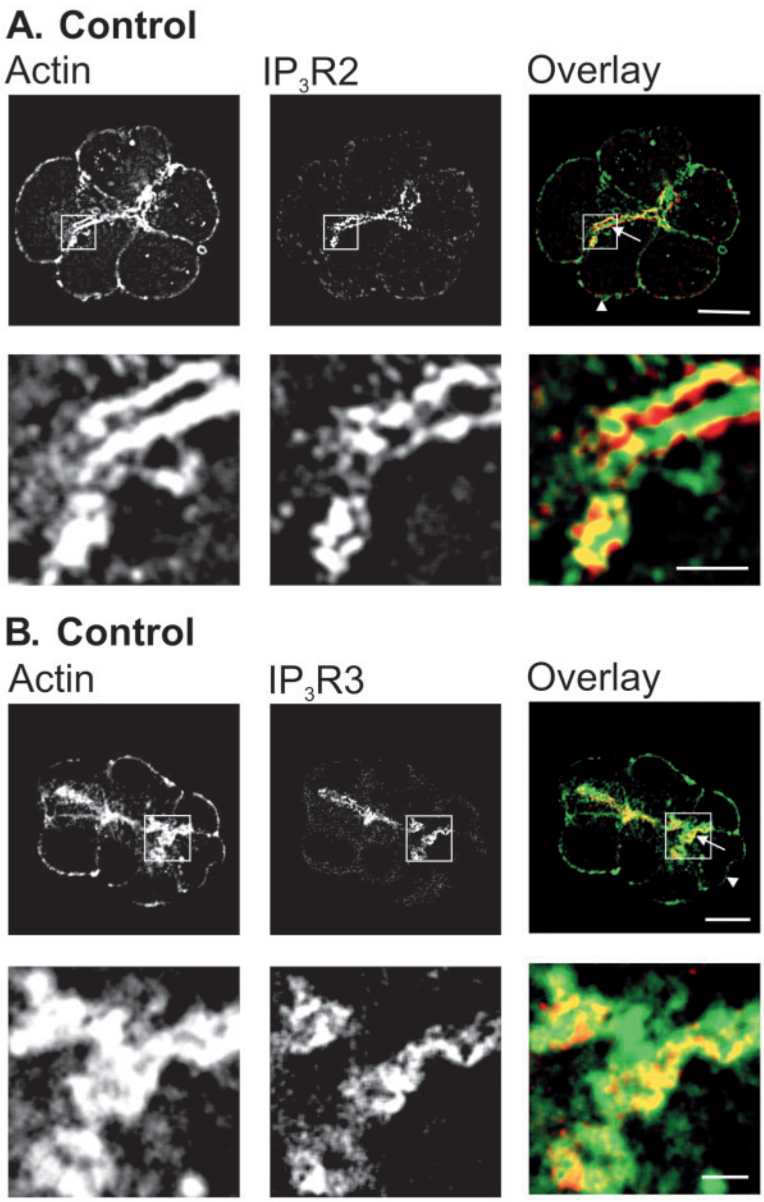

Fig. 2. Actin and IP_3Rs are contained within the same region of the apical subplasamlemmal compartment of pancreatic acini. Isolated pancreatic cell clusters were fixed and stained with (A) antibodies to actin (mAb, green) and IP_3R2 (pAb, red), or (B) antibodies to actin (pAb, green) and IP_3R3 (mAb, red). Images are of confocal sections taken through the middle of the cell clusters. Arrows denote the apical membrane and arrowheads denote the basolateral membrane. Lower panels represent enlarged images of the regions covered by squares. Bar, 10 μm for image of cell cluster and 2 μm for enlarged image.

was observed in the cell cytosol (Fig. 2A,B). However, the predominant immunostaining was found as an enriched band of actin in the cell apex of pancreatic acinar cells, which is similar to the distribution of F-actin seen with phallodin staining (Fig. 2A,B). Co-staining with antibodies to IP_3R2 and IP_3R3 demonstrated that an enriched band of apical actin and IP_3R2 and IP_3R3 are located in the same region of the cell apex (Fig. 2A,B). In addition IP_3R2 staining shows some evidence for receptors in the basal subplasmalemmal regions (Fig. 2A). All images are representative of acquisitions from at least three separate preparations.

Latrunculin B treatment decreases F-actin and induces a loss of IP_3Rs from the apical pole

As F-actin and IP_3Rs were localized in the same cellular compartment of pancreatic acinar cells, experiments were performed to determine whether the F-actin cytoskeleton is involved in localizing IP_3Rs. To investigate this possibility, pancreatic acinar cells were treated with the actin depolymerising agent latrunculin B to determine whether disrupting the F-actin network would lead to a disruption of IP_3R positioning. We have previously used cytochalasin B in an attempt to disrupt the actin cytoskeleton and reported little effect on acinar cells (Fogarty et al., 2000b). However, the mechanism of action of latrunculin B is distinct from that of the cytochalasins (Cooper, 1987). Latrunculin B disrupts the actin cytoskeleton by sequestering G-actin monomers with a 1:1 stoichiometry, thus inhibiting actin polymerisation (Spector et al., 1989).

To determine the effect of latrunculin B on the F-actin network in pancreatic acinar cells, cell clusters were treated with latrunculin B for ~30 minutes and stained with phalloidin (Fig. 3A). There was a clear reduction in F-actin compared to control (cf. Fig. 1A), with an apparent complete loss in F-actin in the subplasmalemmal basolateral regions and a reduction in the dense sub-apical F-actin network. However, a core of F-actin was invariably left within the apical region after treatment, consistent with previous reports (Torgerson and McNiven, 2000). The image in Fig. 3A is representative of acquisitions from at least seven separate preparations.

To quantify these latrunculin B-induced changes in F-actin we used a 10×10 μm region of interest (ROI) and measured the area of phalloidin staining within this box that fell above an arbitrary threshold. A threshold was needed to remove background levels of phalloidin fluorescence (set to remove apparent out-of-cell fluorescence) and was kept constant between control and latrunculin-B-treated images. In control cells, phalloidin staining occupied an area of 54.7 μm^2 within the 100 μm^2 ROI in the apical domain compared with 2.4 μm^2 in a 100 μm^2 ROI in the basolateral domain. After latrunculin B treatment phalloidin staining fell to 25.4±5.5% (mean±s.e.m., n=14) of control levels in the apical domain and 5.7±3.5% (mean±s.e.m., n=14) of control levels in the basolateral domain.

To study the effect of latrunculin B treatment on IP_3R distribution, cell clusters treated with latrunculin B were methanol-fixed and stained with anti-actin and anti-IP_3R antibodies, types 2 and 3. Consistent with the phalloidin-stained cells these cells also displayed a loss of actin (Fig. 3B,C). Inspecting the antibody staining to IP_3R2 (Fig. 3B) and IP_3R3 (Fig. 3C) indicated that in both instances the IP_3R staining was reduced but that in both cases the remaining IP_3R3 staining remained localized to the actin-rich regions. All images are representative of acquisitions from at least three separate preparations. Performing a similar quantification to that for the phalloidin images we found that IP_3R3 within a 10×10 µm ROI in the apical pole occupied an area of 37.5±2.6 μm^2 (*n*=13) above an arbitrary threshold (again set to reduce background fluorescence, i.e. remove out-of-cell fluorescence); IP_3R2 occupied an area of 16.2 μm^2 (*n*=2). Such little staining for IP_3Rs was seen in the basolateral pole that it was not analysed. After latrunculin B treatment the IP_3R3 fluorescence signal in the apical ROI fell to 76.2±6.3% (mean±s.e.m., *n*=46) of the control values and IP_3R2 fluorescence fell to 51.2±7.8 % (mean±s.e.m., *n*=6) of controls.

Since latrunculin B actions rely on sequestration of G-actin monomers we reasoned that agonist stimulation of cells, known to promote actin turnover (Muallem et al., 1995), might exacerbate the effects of latrunculin B. In these experiments we treated the cells with latrunculin B in the presence of 100 µm ACh and also increased the temperature to 37°C. This treatment further reduced the F-actin staining to 1.5±0.8% (mean±s.e.m., *n*=5, phalloidin staining) of control levels and similarly reduced the IP_3R3 staining to 11.3±5.0% (mean±s.e.m., *n*=5, immunostaining). The observations that both IP_3R and F-actin staining were reduced by latrunculin B treatments suggest that IP_3Rs are linked to F-actin.

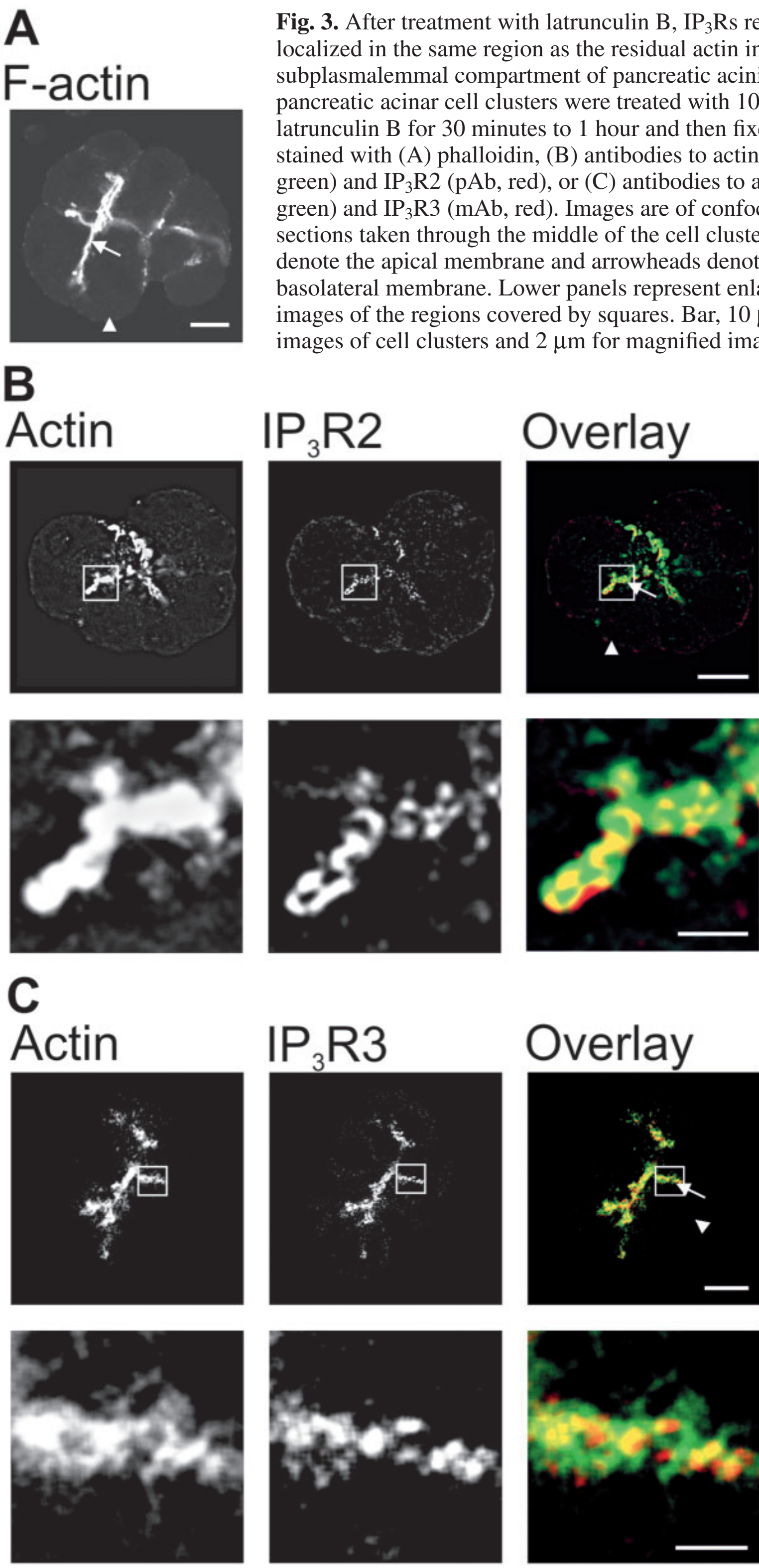

Fig. 3. After treatment with latrunculin B, IP_3Rs remain localized in the same region as the residual actin in the apical subplasmalemmal compartment of pancreatic acini. Isolated pancreatic acinar cell clusters were treated with 100 µM latrunculin B for 30 minutes to 1 hour and then fixed and stained with (A) phalloidin, (B) antibodies to actin (mAb, green) and IP_3R2 (pAb, red), or (C) antibodies to actin (pAb, green) and IP_3R3 (mAb, red). Images are of confocal sections taken through the middle of the cell clusters. Arrows denote the apical membrane and arrowheads denote the basolateral membrane. Lower panels represent enlarged images of the regions covered by squares. Bar, 10 µm for images of cell clusters and 2 µm for magnified image.

Gelsolin primarily disrupts the basolateral F-actin network

In our hands cytochalasins are not very effective at disrupting the F-actin network in acinar cells (Fogarty et al., 2000b). Therefore, to confirm a possible association between F-actin and IP_3Rs, we turned to the endogenous F-actin severing protein gelsolin. Experiments were performed on permeabilized cells with gelsolin added to the permeabilization media either in the absence of Ca^{2+} or in the presence of Ca^{2+}. In the absence of Ca^{2+}, gelsolin is not expected to sever F-actin filaments and phalloidin staining shows the typical pattern of F-actin enrichment in the apical domain with some lesser staining in the subplasmalemmal basolateral regions (Fig. 4, left panel). Application of gelsolin in the presence of Ca^{2+} effectively abolished phalloidin staining in the basal pole to 2.3±1% of control levels (mean±s.e.m., *n*=7) but only marginally reduced the phalloidin staining in the apical pole region (97.1±10.0% of control levels, mean±s.e.m., *n*=7) (Fig. 4, right panel). We conclude that although gelsolin is effective in reducing and fragmenting the basolateral F-actin network the marginal effects in the apical pole preclude its use as a tool to investigate any disruption of apical domain IP_3R distribution.

IP_3Rs are resistant to detergent extraction

If IP_3Rs are linked to the actin cytoskeleton, they might be expected to be resistant to extraction by detergents. A pancreatic homogenate was used to prepare a Triton X-100-insoluble pellet fraction and a Triton X-100-soluble supernatant fraction. The Triton

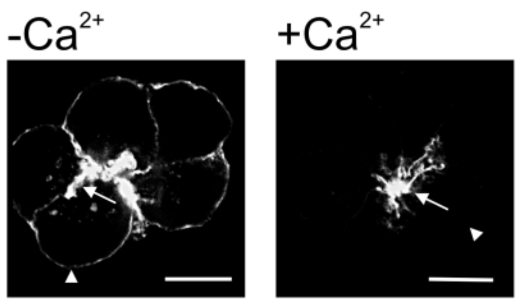

Fig. 4. Gelsolin effects on the actin cytoskeleton in clusters of pancreatic acinar cells. (A) Permeabilized cells were treated for 5 minutes with a BRB80 solution containing 1.3 μM recombinant gelsolin either in the presence of EGTA (left) or in the presence of 1 mM Ca^{2+} (right). Cells were then fixed in paraformaldehyde and stained with phalloidin. We observed gelsolin effects on the F-actin network only in the presence of Ca^{2+}, with a reduction in apical F-actin (arrows) and a substantial loss in the basal pole (arrowheads). Bars, 10 μm.

X-100-insoluble fraction is predicted to be enriched in proteins bound to the cytoskeleton and/or proteins in lipid rafts, whereas the Triton X-100-soluble fraction contains cytosolic proteins and proteins in detergent-solubilized membranes (Gillespie et al., 1989; Shin et al., 2000). Western blot analysis indicated that actin (a band detected of approximately 50 kDa) (Fig. 5A) was present in both the Triton X-100-insoluble pellet (predominately F-actin associated with the plasma membrane), and the Triton X-100-soluble supernatant (predominately monomeric actin within the cytosol). To confirm that our Triton X-100-insoluble pellet was enriched in cytoskeletal proteins, we tested for the distribution of Myosin-IIa, a protein expected to be predominantly associated with the actin cytoskeleton. In the western blots, a band of approximately 250 kDa, consistent with myosin-IIa, was detected only in the Triton X-100-insoluble fraction (Fig. 5B). We conclude that our methods were selectively able to separate proteins associated with the cytoskeleton. Western blot analysis of the IP_3R showed that a band of approximately 220 kDa of similar intensity (measured optical densities gave 53% in the Triton X-100 soluble vs 47% in the insoluble, n=3) in both fractions (Fig. 5C). The western blots were loaded with equal volumes rather than equal proteins and since we loaded 2.73 times as much protein in the Triton X-100 soluble lane, the IP_3R3s are therefore approximately threefold enriched in the Triton X-100-insoluble compartment.

We did attempt experiments using western blot to detect any possible change in the distribution of these proteins after latrunculin B treatment. However, these failed (data not shown) to show any change, most likely a reflection of the experimental protocol that requires use of whole pancreas tissue for the western blots (in order to get enough protein). Under these conditions latrunculin B is likely to affect only the peripheral cells and not the majority of cells deep within the tissue.

Treatment of pancreatic acinar cells with latrunculin B disrupts local Ca^{2+} spiking

To test whether actin disruption had functional effects on IP_3R signalling we used the whole-cell patch-clamp configuration. This allows a precise manipulation of the intracellular environment. Inclusion of 10 μM (2,4,5)IP_3 in the pipette solution initiated spikes of Ca^{2+}-dependent Cl^- current in freshly isolated pancreatic acinar cells. The spikes reflect repetitive, small Ca^{2+} responses restricted to the apical region of the cell (Thorn et al., 1993). This Ca^{2+} response is not easily detectable using conventional imaging methods and therefore whole-cell currents are recorded as a convenient and simple measure of the local Ca^{2+} spikes. Once the whole-cell configuration has been established Ca^{2+}-dependent Cl^- spikes are robust and can continue for extended periods of time (Fig. 6A). The effects of latrunculin B treatment on these spikes were then determined. Prior to the application of latrunculin B a regular pattern of spikes was established. Latrunculin B (50-90 μM) inhibited the current spikes (n=10). These effects were concentration dependent. At 50-67 μM latrunculin B, spikes were still evident within the time range of 5 to 20 minutes in 4 cells, although by the end of each experiment the spikes had either been completely inhibited or reduced in amplitude and altered in profile (Fig. 6Ba). At 90 μM, latrunculin B had completely inhibited spiking within a minute in 75% of cells (Fig. 6C). Given the importance of the actin network in cell physiology, the effect of latrunculin B treatment might be

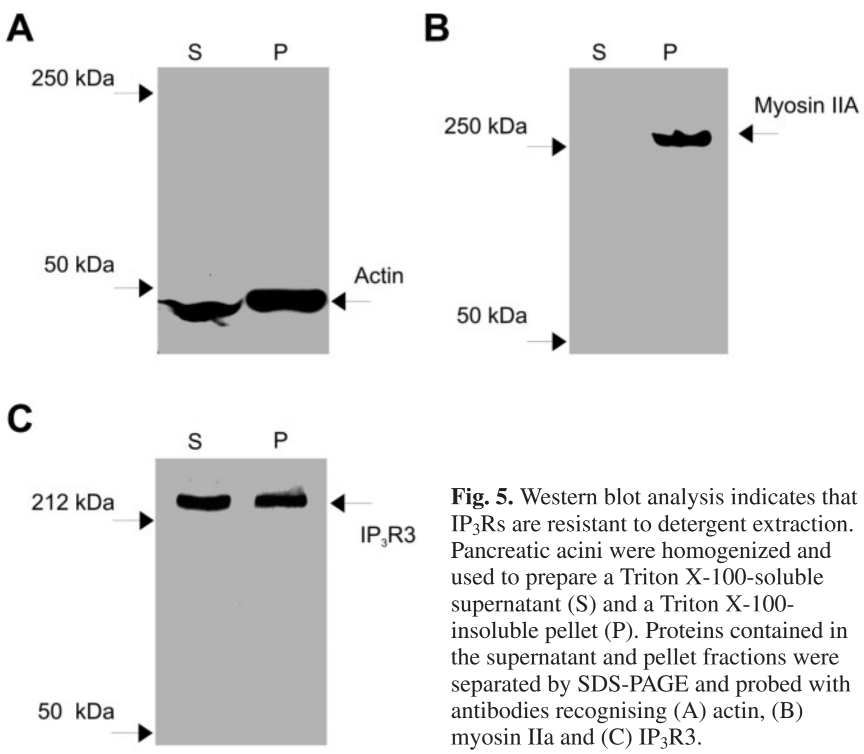

Fig. 5. Western blot analysis indicates that IP_3Rs are resistant to detergent extraction. Pancreatic acini were homogenized and used to prepare a Triton X-100-soluble supernatant (S) and a Triton X-100-insoluble pellet (P). Proteins contained in the supernatant and pellet fractions were separated by SDS-PAGE and probed with antibodies recognising (A) actin, (B) myosin IIa and (C) IP_3R3.

Journal of Cell Science

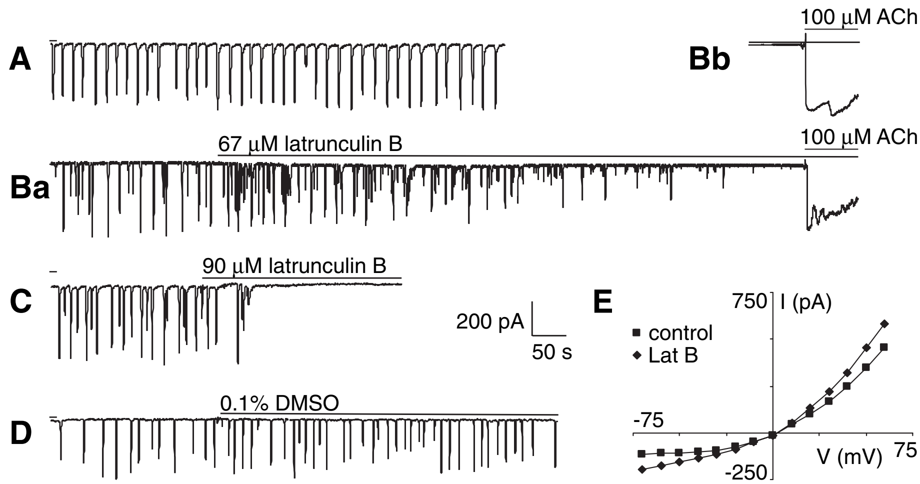

Fig. 6. Latrunculin B inhibits Ca^{2+}-dependent Cl^- current spikes in single whole-cell patch-clamped acinar cells. Cells were held under voltage clamp at a membrane potential of –30 mV. Trains of current spikes (downward deflections in the current, i.e. outward movement of Cl^-) were induced when 10 µM (2,4,5)IP_3 was present in the whole-cell patch pipette (A). Bath application of 50-90 µM latrunculin B led to a dose-dependent cessation of spiking (Ba and C). Application of 100 µM ACh at the end of the recording (Ba) showed the cells were still capable of mobilizing a response even after (2,4,5)IP_3-induced spikes were abolished. The ACh-induced response in the presence of latrunculin B (280±43 pA, mean±s.e.m.) was not different from control responses in the absence of latrunculin B (Bb) (397±57 pA, mean±s.e.m., Student's *t*-test *P*=0.79). DMSO, the drug vehicle, at the maximal concentration used in these experiments had no apparent effect on (2,4,5)IP_3-induced current spikes (D). The horizontal line on the left of the current records is the zero current line. The current-voltage relationship of currents induced by an intracellular solution containing 600 nM Ca^{2+} was not affected by treatment with latrunculin B (E).

nonspecific and reflect a general compromise of cell function. However, we showed that, after latrunculin B had been allowed to inhibit the IP_3-induced spikes, the cells were still able to respond to a supramaximal concentration of ACh (Fig. 6Ba, *n*=7). This response to ACh is not different to the response in control cells (Fig. 6Bb). Addition of dimethylsulfoxide (DMSO), the drug vehicle in which latrunculin B was dissolved, at a concentration used in these experiments (0.1%), had no effect on the current spikes (*n*=4, Fig. 6D). These experiments suggest that latrunculin B inhibits the local Ca^{2+} response. However, another possible interpretation of the inhibition is that latrunculin B has a direct effect on the behaviour of Cl^- channels. To test this we used an intracellular solution containing 600 nM free Ca^{2+} to activate the Cl^- channels directly and therefore bypass mechanisms of Ca^{2+} release. This concentration of Ca^{2+} is known to activate the $Cl_{(Ca)}$ channels maximally (Kidd and Thorn, 2001), and by stepping to a range of membrane potentials we produced current-voltage relationships in control cells and in cells treated with latrunculin B (Fig. 6E). There was no apparent difference in the current-voltage relationship after latrunculin B treatment indicating that the drug has no direct effect on channel behaviour. To distinguish further the effects of latrunculin B on the current spikes, patch clamp experiments were combined with Ca^{2+} imaging to allow us to measure any effect on the Ca^{2+} signal directly.

By combining patch clamp and Ca^{2+} imaging experiments it was possible to show that the loss of the current spikes shown in Fig. 6 was due to an inhibition of the underlying Ca^{2+} signal. Fig. 7A demonstrates that latrunculin B (*n*=3, 25-90 µM) causes an inhibition in (2,4,5)IP_3-evoked Cl^- current spiking in freshly isolated pancreatic acinar cells in accordance with previous data. At time points i-v the local Ca^{2+} response was also measured by imaging the Ca^{2+} indicator Calcium Green that had been included in the pipette solution. Fig. 7B shows the average Ca^{2+} response (denoted by an asterisk) at time points i-v. As can be seen over the time course of the experiment the Ca^{2+} response diminishes, which coincides with a reduction of current spiking. The corresponding pseudocolour fluorescence ratio images at time points i-v are also shown. Before the addition of latrunculin B there is a clear Ca^{2+} response that emanates from close to the apical membrane and at its peak is restricted to the apical region of the cell. After the addition of latrunculin B there is a gradual reduction in the response, although it still emanates from close to the apical membrane and is restricted to the apical region of the cell. Therefore, the data presented here demonstrate that latrunculin B disrupts local Ca^{2+} spiking induced by (2,4,5)IP_3 in pancreatic acinar cells.

Discussion

The experiments described in this study indicate that IP_3R2 and IP_3R3 and the F-actin network are all enriched within the same apical subplasmalemmal compartment in mouse pancreatic acinar cells. Treatment with latrunculin B reduced the basolateral and apical subplasmalemmal F-actin network; IP_3R distribution was also reduced, but the IP_3Rs remaining in the apical domain were always associated with the remaining F-actin. Western blot analysis demonstrated that IP_3Rs are resistant to detergent extraction suggesting a possible attachment to the cytoskeleton. Finally, treatment of isolated pancreatic acinar cells with latrunculin B inhibited local but not global Ca^{2+} signals. Taken together these results suggest that F-actin forms links with IP_3Rs in the apical subplasmalemmal compartment and this positioning is important for the generation of local Ca^{2+} signals.

Evidence for a physical link between the actin cytoskeleton and IP_3Rs

Here we show that a population of IP_3Rs are resistant to detergent extraction (Fig. 5A). Furthermore, immunocytochemistry demonstrates that F-actin is contained within the same apical compartment as IP_3R2 and IP_3R3 (Figs 1, 2), which suggests that the IP_3R detergent insolubility is

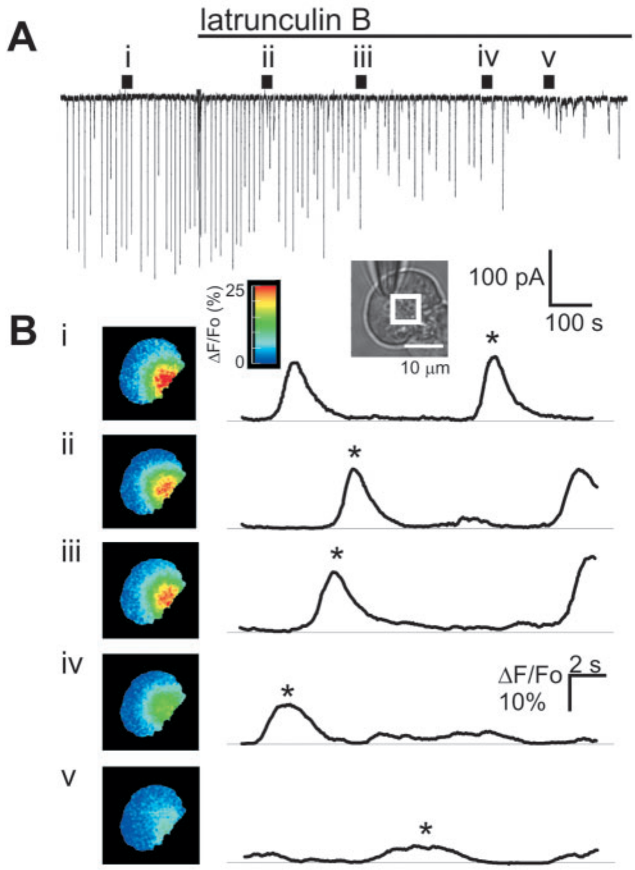

Fig. 7. Inhibitory effects of latrunculin B on Ca^{2+}-dependent Cl^- current spikes are mediated by an inhibition of the underlying local Ca^{2+} signal. Latrunculin B inhibits Ca^{2+}-dependent Cl^- current spikes induced by (2,4,5)IP_3 in whole-cell patch-clamped pancreatic acinar cells (A). At time points i-v shown in the patch-clamp trace the average Ca^{2+} signal, denoted by an asterisk and measured within the white box shown in the phase image, was measured (B). The pseudocolour fluorescence ratio image at these times is also shown.

caused by IP_3Rs forming links, directly or indirectly, with F-actin.

A number of reports have proposed a physical interaction between IP_3Rs and the actin cytoskeleton based on the detergent insolubility of a population of IP_3Rs (Guillemette et al., 1990; Joseph and Samanta, 1993). In line with this hypothesis, it has been shown that the actin cytoskeleton can be co-immunoprecipitated with IP_3Rs in smooth muscle cells (Sugiyama et al., 2000) and, more relevantly, in pancreatic acinar cells (Giovannucci et al., 2000).

The nature of these links to the actin cytoskeleton are not known but a number of reports suggest it is indirect via accessory proteins. In smooth muscle cells IP_3Rs co-immunoprecipitate with talin, an actin-binding protein localized to focal adhesions (Sugiyama et al., 2000). It has also been proposed that ankyrin, another actin-binding protein, functionally interacts with the IP_3R (Bourguignon and Jin, 1995; Joseph and Samanta, 1993), and that in ankyrin knock-out mice IP_3Rs are mislocalized in cardiomyocytes and thymus (Tuvia et al., 1999). Another candidate for linking IP_3Rs to the actin network is myosin II, identified by a yeast two-hybrid screen in *C. elegans* (Walker et al., 2002). Finally, the scaffold protein Homer has been shown to link to IP_3Rs and the actin cytoskeleton in neuronal postsynaptic spines (Tu et al., 1998; Tu et al., 1999).

Evidence for such associations in pancreatic acinar cells is not available except for a recent study demonstrating that Homer subtypes 1 and 2 are present in the apical subplasmalemmal region (Shin et al., 2003). However, in Homer-2-knockout mice the distribution of all known types of IP_3R was unaffected.

How does disruption of the F-actin network affect the local Ca^{2+} signals?

There are a number of possible targets to explain latrunculin B inhibition of local Ca^{2+} signals. G-protein-coupled receptors are known to bind to actin-associated proteins (Burgueño et al., 2003; Enz, 2002; Lin et al., 2001) and disruption of the actin cytoskeleton could have an inhibitory effect on the signal transduction pathways. However, the method used in our study delivers (2,4,5)IP_3 to elicit local Ca^{2+} spikes directly, and therefore the effects of latrunculin B cannot be mediated through an action on cell-surface receptors (Shin et al., 2001). Disruption of the actin cytokeleton has been shown to inhibit Ca^{2+} entry in vascular endothelial cells (Holda and Blatter, 1997), astrocytes (Grimaldi et al., 1999) and platelets (Rosado and Sage, 2000). However, it is unlikely that the effects of latrunculin B on the local Ca^{2+} response that were measured in our study are due to a block of Ca^{2+} entry as the local Ca^{2+} response is largely independent of extracellular Ca^{2+} (Wakui et al., 1989). Another way in which latrunculin B could effect the local Ca^{2+} response is through an action on the plasma membrane Ca^{2+}-ATPase (PMCA), which plays an integral role in the formation of complex patterns of Ca^{2+} signals measured in pancreatic acinar cells (Petersen et al., 1999). PMCA is present at the luminal plasma membrane of pancreatic acinar cells (Lee et al., 1997a) and may associate with the actin cytoskeleton in large subplasmalemmal complexes (Shin et al., 2000). However, our control experiments show that after latrunculin-B-induced loss of Ca^{2+} spiking the cells are still capable of responding to high concentrations of ACh (Fig. 6Ba). This indicates that Ca^{2+} stores are still intact and suggests that there is no gross effect on cellular Ca^{2+} handling that might be expected if the PMCA activity was blocked. We conclude that none of these possibilities provides a plausible explanation for the actions of latrunculin B on the local Ca^{2+} spike.

Instead, we suggest that latrunculin B action on the local positioning of IP_3Rs in the apical region leads directly to a loss of the local Ca^{2+} response. We have previously shown that the generation of a local Ca^{2+} response is dependent on the coordinated activity of a small number (2-3) of discrete Ca^{2+} release sites within the apical pole (Thorn et al., 1996; Kidd et al., 1999). Introduction of exogenous Ca^{2+} buffers disrupted the local Ca^{2+} response in a manner consistent with an essential role for Ca^{2+}-induced Ca^{2+} release acting as a signal recruiting and coordinating Ca^{2+} release from each discrete site (Kidd et al., 1999). We suggest that latrunculin B treatment reduces the apical location of IP_3Rs, initially reducing the size of the Ca^{2+} spikes, and that eventually, when IP_3R numbers drop below a critical threshold, a loss of Ca^{2+}-induced Ca^{2+} release leads to an abolition of local Ca^{2+} spikes. Since the IP_3Rs are still present in the cell the subsequent presentation of a supramaximal agonist concentration leads to the recruitment of all IP_3Rs and leads to the global Ca^{2+} response we observe (Fig. 6Ba).

Implications for F-actin turnover in pancreatic acinar cells

We show that latrunculin B treatment essentially removes F-actin from the basal pole but still leaves some residual F-actin in the apical pole, an observation consistent with a previous report of a recalcitrant pool of F-actin (Torgerson and McNiven, 2000). However, we now show that, in the presence of an agonist and with an increased temperature, a 1 hour treatment with latrunculin B considerably reduces this residual apical F-actin. We conclude that pancreatic acinar cells have a labile pool of F-actin, which is readily affected by latrunculin B, and an apical F-actin pool, which has a slower turnover and confers a measure of latrunculin B resistance. Consistent with this, it has been reported that the F-actin cytoskeleton in other cell types may consist of two distinct pools, one stable and the other dynamic (Fischer et al., 1998; Halpain, 2000; Ammar et al., 2001; Star et al., 2002). In pancreatic acinar cells F-actin remodelling is thought to occur in response to agonist stimulation, which demonstrates the need for a dynamic pool (Bauduin et al., 1975; Muallem et al., 1995; Valentijn et al., 2000); it is possible that a more stable F-actin pool plays a role in other cellular processes.

Conclusions

In conclusion, our data indicate that F-actin is linked to IP_3Rs within an apical subplasmalemmal complex in pancreatic acinar cells. Disruption of the actin network with latrunculin B leads to a loss of local Ca^{2+} spiking, which suggests that this link serves to localize Ca^{2+} release sites within the apical subplasmalemmal region. This arrangement may ensure the efficient activation of Ca^{2+}-dependent machinery involved in the regulation of enzyme and fluid secretion.

M.R.T. was in receipt of a Biotechnology and Biological Sciences Research Council PhD studentship. Work in the laboratory was supported with a Medical Research Council grant G000024.

References

Ammar, D. A., Nguyen, P. N. and Forte, J. G. (2001). Functionally distinct pools of actin in secretory cells. *Am. J. Physiol. Cell Physiol.* **281**, C407-C417.

Bauduin, H., Stock, C., Vincent, D. and Grenier, J. F. (1975). Microfilamentous system and secretion of enzyme in the exocrine pancreas. Effect of cytochalasin B. *J. Cell Biol.* **66**, 165-181.

Berridge, M. J. (1993). Inositol trisphosphate and calcium signalling. *Nature* **361**, 315-325.

Bourguignon, L. Y. and Jin, H. (1995). Identification of the ankyrin-binding domain of the mouse T-lymphoma cell inositol 1,4,5-trisphosphate IP_3 receptor and its role in the regulation of IP_3-mediated internal Ca^{2+} release. *J. Biol. Chem.* **270**, 7257-7260.

Bourguignon, L. Y., Iida, N. and Jin, H. (1993a). The involvement of the cytoskeleton in regulating IP_3 receptor-mediated internal Ca^{2+} release in human blood platelets. *Cell Biol. Int.* **17**, 751-758.

Bourguignon, L. Y., Jin, H., Iida, N., Brandt, N. R. and Zhang, S. H. (1993b). The involvement of ankyrin in the regulation of inositol 1,4,5-trisphosphate receptor-mediated internal Ca^{2+} release from Ca^{2+} storage vesicles in mouse T-lymphoma cells. *J. Biol. Chem.* **268**, 7290-7297.

Burgueño, J., Blake, D. J., Benson, M. A., Tinsley, C. L., Esapa, C. T., Canela, E. I., Penela, P., Mallol, J., Mayor, F., Jr, Lluis, C., Franco, R. and Ciruela, F. (2003). The adenosine A_{2A} receptor interacts with the actin-binding protein α-actinin. *J. Biol. Chem.* **278**, 37545-37552.

Cooper, J. A. (1987). Effects of cytochalasin and phalloidin on actin. *J. Cell Biol.* **105**, 1473-1478.

Enz, R. (2002). The actin-binding protein Filamin-A interacts with the metabotropic glutamate receptor type 7. *FEBS Lett.* **514**, 184-188.

Fischer, M., Kaech, S., Knutti, D. and Matus, A. (1998). Rapid actin-based plasticity in dendritic spines. *Neuron* **20**, 847-854.

Fogarty, K. E., Kidd, J. F., Tuft, D. A. and Thorn, P. (2000a). Mechanisms underlying $InsP_3$-evoked global Ca^{2+} signals in mouse pancreatic acinar cells. *J. Physiol.* **526**, 515-526.

Fogarty, K. E., Kidd, J. F., Turner, A., Skepper, J. N., Carmichael, J. and Thorn, P. (2000b). Microtubules regulate local Ca^{2+} spiking in secretory epithelial cells. *J. Biol. Chem.* **275**, 22487-22494.

Gillespie, C. S., Wilson, R., Davidson, A. and Brophy, P. J. (1989). Characterization of a cytoskeletal matrix associated with myelin from rat brain. *Biochem. J.* **260**, 689-696.

Giovannucci, D. R., Yule, D. I. and Stuenkel, E. L. (1998). Optical measurement of stimulus-evoked membrane dynamics in single pancreatic acinar cells. *Am. J. Physiol.* **275**, C732-C739.

Giovannucci, D. R., Groblewski, G. E., Sneyd, J. and Yule, D. I. (2000). Targeted phosphorylation of inositol 1,4,5-trisphosphate receptors selectively inhibits localized Ca^{2+} release and shapes oscillatory Ca^{2+} signals. *J. Biol. Chem.* **275**, 33704-33711.

Grimaldi, M., Favit, A. and Alkon, D. L. (1999). cAMP-induced cytoskeleton rearrangement increases calcium transients through the enhancement of capacitative calcium entry. *J. Biol. Chem.* **274**, 33557-33564.

Guillemette, G., Favreau, I., Boulay, G. and Potier, M. (1990). Solubilization and partial characterization of inositol 1,4,5-trisphosphate receptor of bovine adrenal cortex reveal similarities with the receptor of rat cerebellum. *Mol. Pharmacol.* **38**, 841-847.

Halpain, S. (2000). Actin and the agile spine: how and why do dendritic spines dance? *Trends Neurosci* **23**, 141-146.

Hamill, O. P., Marty, A., Neher, E., Sakmann, B. and Sigworth, F. J. (1981). Improved patch-clamp techniques for high-resolution current recording from cells and cell-free membrane patches. *Pflügers Arch.* **391**, 85-100.

Holda, J. R. and Blatter, L. A. (1997). Capacitative calcium entry is inhibited in vascular endothelial cells by disruption of cytoskeletal microfilaments. *FEBS Lett.* **403**, 191-196.

Ito, K., Miyashita, Y. and Kasai, H. (1997). Micromolar and submicromolar Ca^{2+} spikes regulating distinct cellular functions in pancreatic acinar cells. *EMBO J.* **16**, 242-251.

Joseph, S. K. and Samanta, S. (1993). Detergent solubility of the inositol trisphosphate receptor in rat brain membranes. Evidence for association of the receptor with ankyrin. *J. Biol. Chem.* **268**, 6477-6486.

Kasai, H. and Augustine, G. J. (1990). Cytosolic Ca^{2+} gradients triggering unidirectional fluid secretion from exocrine pancreas. *Nature* **348**, 735-738.

Kasai, H., Li, Y. X. and Miyashita, Y. (1993). Subcellular distribution of Ca^{2+} release channels underlying Ca^{2+} waves and oscillations in exocrine pancreas. *Cell* **74**, 669-677.

Kidd, J. F. and Thorn, P. (2001). The properties of the secretagogue-evoked chloride current in mouse pancreatic acinar cells. *Pflugers Arch.* **441**, 489-497.

Kidd, J. F., Fogarty, K. E., Tuft, R. A. and Thorn, P. (1999). The role of Ca^{2+} feedback in shaping $InsP_3$-evoked Ca^{2+} signals in mouse pancreatic acinar cells. *J. Physiol.* **520**, 187-201.

Lee, M. G., Xu, X., Zeng, W., Diaz, J., Kuo, T. H., Wuytack, F., Racymaekers, L. and Muallem, S. (1997a). Polarized expression of Ca^{2+} pumps in pancreatic and salivary gland cells. Role in initiation and propagation of $[Ca^{2+}]_i$ waves. *J. Biol. Chem.* **272**, 15771-15776.

Lee, M. G., Xu, X., Zeng, W., Diaz, J., Wojcikiewicz, R. J., Kuo, T. H., Wuytack, F., Racymaekers, L. and Muallem, S. (1997b). Polarized expression of Ca^{2+} channels in pancreatic and salivary gland cells. Correlation with initiation and propagation of $[Ca^{2+}]_i$ waves. *J. Biol. Chem.* **272**, 15765-15770.

Lin, R., Karpa, K., Kabbani, N., Goldman-Rakic, P. and Levenson, R. (2001). Dopamine D2 and D3 receptors are linked to the actin cytoskeleton via interaction with filamin A. *Proc. Natl. Acad. Sci. USA* **98**, 5258-5263.

Muallem, S., Kwiatkowska, K., Xu, X. and Yin, H. L. (1995). Actin filament disassembly is a sufficient final trigger for exocytosis in nonexcitable cells. *J. Cell Biol.* **128**, 589-598.

Nathanson, M. H., Fallon, M. B., Padfield, P. J. and Maranto, A. R. (1994). Localization of the type 3 inositol 1,4,5-trisphosphate receptor in the Ca^{2+} wave trigger zone of pancreatic acinar cells. *J. Biol. Chem.* **269**, 4693-4696.

Palade, G. (1975). Intracellular aspects of the process of protein synthesis. *Science* **189**, 347-358.

Park, M. K., Lomax, R. B., Tepikin, A. V. and Petersen, O. H. (2001). Local uncaging of caged Ca^{2+} reveals distribution of Ca^{2+}-activated Cl^- channels in pancreatic acinar cells. *Proc. Natl. Acad. Sci. USA* **98**, 10948-10953.

Petersen, O. H. (1992). Stimulus-secretion coupling: cytoplasmic calcium signals and the control of ion channels in exocrine acinar cells. *J. Physiol.* **448**, 1-51.

Petersen, O. H., Burdakov, D. and Tepikin, A. V. (1999). Polarity in intracellular calcium signaling. *Bioessays* **21**, 851-860.

Rizzuto, R., Pinton, P., Carrington, W., Fay, F. S., Fogarty, K. E., Lifshitz, L. M., Tuft, R. A. and Pozzan, T. (1998). Close contacts with the endoplasmic reticulum as determinants of mitochondrial Ca^{2+} responses. *Science* **280**, 1763-1766.

Rosado, J. A. and Sage, S. O. (2000). Farnesylcysteine analogues inhibit store-regulated Ca^{2+} entry in human platelets: evidence for involvement of small GTP-binding proteins and actin cytoskeleton. *Biochem. J.* **347**, 183-192.

Rossier, M. F., Bird, G. S. and Putney, J. W., Jr (1991). Subcellular distribution of the calcium-storing inositol 1,4,5-trisphosphate-sensitive organelle in rat liver. Possible linkage to the plasma membrane through the actin microfilaments. *Biochem. J.* **274**, 643-650.

Shin, D. M., Zhao, X. S., Zeng, W., Mozhayeva, M. and Muallem, S. (2000). The mammalian Sec6/8 complex interacts with Ca^{2+} signaling complexes and regulates their activity. *J. Cell Biol.* **150**, 1101-1112.

Shin, D. M., Luo, X., Wilkie, T. M., Miller, L. J., Peck, A. B., Humphreys-Beher, M. G. and Muallem, S. (2001). Polarized expression of G protein-coupled receptors and an all-or-none discharge of Ca^{2+} pools at initiation sites of $[Ca^{2+}]_i$ waves in polarized exocrine cells. *J. Biol. Chem.* **276**, 44146-44156.

Shin, D. M., Dehoff, M., Luo, X., Kang, S. H., Tu, J., Nayak, S. K., Ross, E. M., Worley, P. F. and Muallem, S. (2003). Homer 2 tunes G protein-coupled receptors stimulus intensity by regulating RGS proteins and PLC? GAP activities. *J. Cell Biol.* **162**, 293-303.

Spector, I., Shochet, N. R., Blasberger, D. and Kashman, Y. (1989). Latrunculins-novel marine macrolides that disrupt microfilament organization and affect cell growth: I. Comparison with cytochalasin D. *Cell Motil. Cytoskeleton* **13**, 127-144.

Star, E. N., Kwiatkowski, D. J. and Murthy, V. N. (2002). Rapid turnover of actin in dendritic spines and its regulation by activity. *Nat. Neurosci.* **5**, 239-246.

Stecher, B., Ahnert-Hilger, G., Weller, U., Kemmer, T. P. and Gratzl, M. (1992). Amylase release from streptolysin O-permeabilized pancreatic acinar cells. Effects of Ca^{2+}, guanosine 5′-[gamma-thio]triphosphate, cyclic AMP, tetanus toxin and botulinum A toxin. *Biochem. J.* **283**, 899-904.

Streb, H., Irvine, R. F., Berridge, M. J. and Schulz, I. (1983). Release of Ca^{2+} from a nonmitochondrial intracellular store in pancreatic acinar cells by inositol-1,4,5-trisphosphate. *Nature* **306**, 67-69.

Sugiyama, T., Matsuda, Y. and Mikoshiba, K. (2000). Inositol 1,4,5-trisphosphate receptor associated with focal contact cytoskeletal proteins. *FEBS Lett.* **466**, 29-34.

Thorn, P. and Petersen, O. H. (1992). Activation of nonselective cation channels by physiological cholecystokinin concentrations in mouse pancreatic acinar cells. *J. Gen. Physiol.* **100**, 11-25.

Thorn, P., Lawrie, A. M., Smith, P. M., Gallacher, D. V. and Petersen, O. H. (1993). Local and global cytosolic Ca^{2+} oscillations in exocrine cells evoked by agonists and inositol trisphosphate. *Cell* **74**, 661-668.

Thorn, P., Moreton, R. and Berridge, M. (1996). Multiple, coordinated Ca^{2+}-release events underlie the inositol trisphosphate-induced local Ca^{2+} spikes in mouse pancreatic acinar cells. *EMBO J.* **15**, 999-1003.

Torgerson, R. R. and McNiven, M. A. (2000). Agonist-induced changes in cell shape during regulated secretion in rat pancreatic acini. *J. Cell Physiol.* **182**, 438-447.

Tu, J. C., Xiao, B., Yuan, J. P., Lanahan, A. A., Leoffert, K., Li, M., Linden, D. J. and Worley, P. F. (1998). Homer binds a novel proline-rich motif and links group 1 metabotropic glutamate receptors with IP3 receptors. *Neuron* **21**, 717-726.

Tu, J. C., Xiao, B., Naisbitt, S., Yuan, J. P., Petralia, R. S., Brakeman, P., Doan, A., Aakalu, V. K., Lanahan, A. A., Sheng, M. et al. (1999). Coupling of mGluR/Homer and PSD-95 complexes by the Shank family of postsynaptic density proteins. *Neuron* **23**, 583-592.

Tuvia, S., Buhusi, M., Davis, L., Reedy, M. and Bennett, V. (1999). Ankyrin-B is required for intracellular sorting of structurally diverse Ca^{2+} homeostasis proteins. *J. Cell Biol.* **147**, 995-1008.

Valentijn, J. A., Valentijn, K., Pastore, L. M. and Jamieson, J. D. (2000). Actin coating of secretory granules during regulated exocytosis correlates with the release of rab3D. *Proc. Natl. Acad. Sci. USA* **97**, 1091-1095.

Wakui, M., Potter, B. V. and Petersen, O. H. (1989). Pulsatile intracellular calcium release does not depend on fluctuations in inositol trisphosphate concentration. *Nature* **339**, 317-320.

Walker, D. S., Ly, S., Lockwood, K. C. and Baylis, H. A. (2002). A direct interaction between IP_3 receptors and myosin II regulates IP_3 signaling in C. elegans. *Curr. Biol.* **12**, 951-956.

Williams, J. A. (2001). Intracellular signaling mechanisms activated by cholecystokinin-regulating synthesis and secretion of digestive enzymes in pancreatic acinar cells. *Annu. Rev. Physiol.* **63**, 77-97.

Williams, J. A., Groblewski, G. E., Ohnishi, H. and Yule, D. I. (1997). Stimulus-secretion coupling of pancreatic digestive enzyme secretion. *Digestion* **58 Suppl. 1**, 42-45.

Wojcikiewicz, R. J. (1995). Type I, II, and III inositol 1,4,5-trisphosphate receptors are unequally susceptible to down-regulation and are expressed in markedly different proportions in different cell types. *J. Biol. Chem.* **270**, 11678-11683.

Yule, D. I., Ernst, S. A., Ohnishi, H. and Wojcikiewicz, R. J. (1997). Evidence that zymogen granules are not a physiologically relevant calcium pool. Defining the distribution of inositol 1,4,5-trisphosphate receptors in pancreatic acinar cells. *J. Biol. Chem.* **272**, 9093-9098.